Midinfrared intersubband electroluminescence of Si/SiGe quantum cascade structures

I. Bormann,[a] K. Brunner, S. Hackenbuchner, G. Zandler, and G. Abstreiter
Walter Schottky Institut, Technische Universität München, Am Coulombwall, D-85748 Garching, Germany

S. Schmult and W. Wegscheider
Institut für Angewandte und Experimentelle Physik, Universität Regensburg, D-93040 Regensburg, Germany

(Received 29 October 2001; accepted for publication 29 January 2002)

Unipolar intersubband lasers like quantum cascade laser structures might be realized not only in III–V semiconductors but also in Si/SiGe multiple layer structures since no optical transitions across the indirect band gap are involved. We report on well-defined intersubband electroluminescence emission of Si/SiGe quantum cascade structures with different active quantum wells parameters. The complex valence band structure and a nonradiative relaxation rate of about 400 fs were calculated by multiband $k \cdot p$ formalism including Si/Ge segregation effects. The observed spectral shift of the electroluminescence peak from 146 to 159 meV is described well by quantum confinement of the two lowest heavy hole subbands. The electroluminescence observed reveals transverse magnetic polarization, a spectral line shape that changes with the direction of the current, and low-energy line broadening with an increase in temperature and current. All these features are described well by the $k \cdot p$ model calculation. © *2002 American Institute of Physics.*
[DOI: 10.1063/1.1465131]

Since silicon is the dominant semiconductor in microelectronics, it would be highly desirable to realize silicon based light emitters for integrating optical and microelectronic components on the same chip. In unipolar lasers like quantum cascade lasers (QCLs),[1] the most important obstacle to silicon based light emitters—the indirect band gap—is irrelevant, since the radiative transition occurs within subbands of the same band. This opens the possibility of realizing a QCL device in silicon–germanium technology. In the Si/SiGe system carriers can be confined in the valence as well as in the conduction band, depending upon the strain configuration.[2] However, to achieve confinement potential in the conduction band, growth of a relaxed SiGe buffer is necessary, whereas for pseudomorphic growth on a Si substrate most of the band offset occurs in the valence band. In this case the cascading scheme has to be implemented using holes in the valence band (VB), in contrast to all existing QCLs based on III–V semiconductors that all employ electron cascade structures.[1,3,4] Electroluminescence from such a SiGe quantum cascade structure grown on Si has recently been demonstrated.[5]

In this letter we present results of SiGe QC structures with quantum confinement shift of the electroluminescence peak and detailed $k \cdot p$ model calculations. We have designed and fabricated two SiGe quantum cascade structures with varied active regions that reveal wavelengths around 8 μm. The peak shift is attributed to the shift of the heavy hole subband energies by quantum confinement. We did a thorough calculation of the Si/SiGe band structure using multiband $k \cdot p$ envelope function theory. This not only allows one to predict the emission wavelength exactly but also accounts for the experimentally observed asymmetric line broadening due to in-plane energy dispersion. A calculation of the nonradiative scattering rates yields the path of main nonradiative relaxation.

For the band structure calculation we used the parameters given in Ref. 2. Strain in the materials was calculated within the elasticity theory. Because Ge is known to show significant segregation at growth temperatures above 350 °C,[6,7] we included a two-state exchange kinetic model to describe segregation effects in the actual Ge profile of the Si/SiGe multilayers using the parameters determined by Fukatsu *et al.*[8] We have in addition calculated the depopulation time of the heavy hole (HH)2 subband due to optical deformation potential scattering. The hole–phonon matrix element $\langle i|D \cdot u|f\rangle$ was evaluated where $|i\rangle$ and $|f\rangle$ denote the initial and final hole states from the $k \cdot p$ band structure and D denotes the deformation potential tensor described in Ref. 9. The scattering time is obtained by applying Fermi's golden rule and integrating over all final states. For atomic displacements u we assumed a weighted alloy (optical) phonon spectrum consisting of Si–Si (64.3 meV), Si–Ge (50.8 meV) and Ge–Ge (37.4 meV) modes.[10]

Both structures realize a VB quantum cascade structure based on a vertical radiative transition from the HH2 to the HH1 ground state within a single quantum well. Figure 1 shows the band structure of our first structure (S1). The layer thicknesses and corresponding Ge contents are given in the Fig. 1 caption. Holes are injected from the lowest HH subband of the quantum well (QW)7 into the HH2 level of active QW1, where a radiative transition into the HH1 state should take place. QW2–5 are chosen to form a miniband of heavy hole levels to extract holes from the HH1 level of the active well. A minigap for HH as well as for light hole (LH) states prevents the tunneling of holes into continuum states. To minimize space charge effects, the center layers of the

[a]Author to whom correspondence should be addressed; electronic mail: ingo.bormann@wsi.tu-muenchen.de

 © 2002 American Institute of Physics
Downloaded 27 Aug 2002 to 129.187.9.4. Redistribution subject to AIP license or copyright, see http://ojps.aip.org/aplo/aplcr.jsp

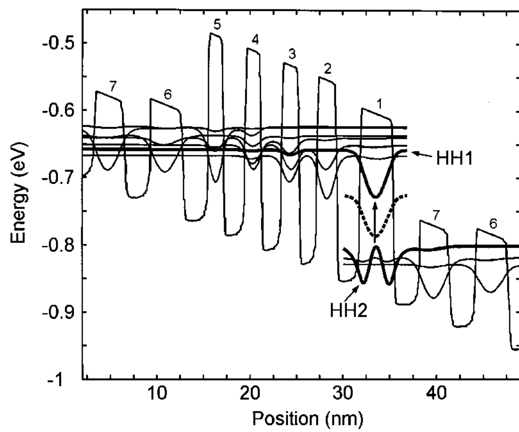

FIG. 1. Calculated band structure of sample S1 with an applied electric field of 55 kV/cm. Shown are the HH potential, HH states (solid lines) and LH/SO states (dotted lines) for $k_{II}=0$. The layer thickness (Å) and Ge contents of the QW and of Si barriers 1–7 are 38/0.4, 23/0, 23/0.43, 18/0, 21/0.43, 20/0, 19/0.43, 22/0, 17/0.43, 24/0, 38/0.24, 24/0, 35/0.21, and 26/0. The QWs and barriers 4–6 are 7×10^{17} cm^{-3} p doped with boron.

superlattice region are doped with boron to $p=7\times10^{17}$ cm^{-3}. Our second structure (S2) is very similar to structure 1, but all wells contain 5% more Ge, the thickness of the active well is slightly decreased and one additional well is inserted between wells 7 and 1 in order to match the design of the cascade. The average Ge contents of 18% (S1) and 19% (S2) are close to the metastable thickness limit for strain relaxation given by Dodson and Tsao.[11]

The structures were grown on a 2×10^{16} cm^{-3} p-doped (100) Si substrate at 480 °C with a Riber molecular beam epitaxy (MBE) system. The sample consists of 15 cascade periods. 98 nm p-Si (1×10^{18} cm^{-3}) spacer layers after every third cascade keep the average strain moderate. The top contact consists of 200 nm p-Si (4×10^{18} cm^{-3}) and 30 nm p^+-Si (3×10^{19} cm^{-3}) with evaporated Al/Au films. The second contact is at the back side of the wafer. The samples were processed into (410 μm)^2 mesas and a 60° facet was polished close to the mesa to couple out light.

A transmission electron microscopy (TEM) analysis of our structures indicates no strain relaxation from dislocations or layer waviness in the regions studied. Figure 2 shows a high resolution image of S1. The thickness of one period corresponds within 3% to the nominal growth parameters. The interface roughness of the layers is limited to at most 3 monolayers. The leading edge of the QWs in the growth direction seems to be better defined than the trailing edge as was predicted by the segregation model[7] and as modeled in the HH potential in Fig. 1.

Electroluminescence (EL) measurements were performed with a Fourier transform infrared (FTIR) Nicolet spectrometer using a step scan and lock-in detection technique. Emission was detected by a liquid-nitrogen-cooled HgCdTe detector. The samples were mounted in a He-flow cryostat. The EL measurements were performed with two adjacent mesas pumped in parallel at a pulse repetition period of 10.7 μs at varying duty cycles.

Figure 3 shows EL spectra of both structures at a nominal heat sink temperature of 20 K. The sample's temperature is expected to be significantly higher due to thermal heating by current at high duty cycles. Structure S1 emits EL at 146 meV with a linewidth of about 30 meV, in good agreement with our calculated HH2–HH1 transition energy of 143 meV. The second structure, S2, emits about the same EL intensity, but the peak is centered at higher energy of 159 meV. This energy is again in very good agreement with our calculated transition energy of 163 meV. The EL blueshift of S2 is due to the stronger quantum confinement of sample S2 caused by the reduction in thickness of the active QW by 3 Å and the 5% increase in Ge content in all wells. The observed linewidth is as low as 23 meV. Polarization-dependent spectra show clear transverse magnetic (TM) polarization as is expected from optical selection rules for transitions between HH subbands.[12]

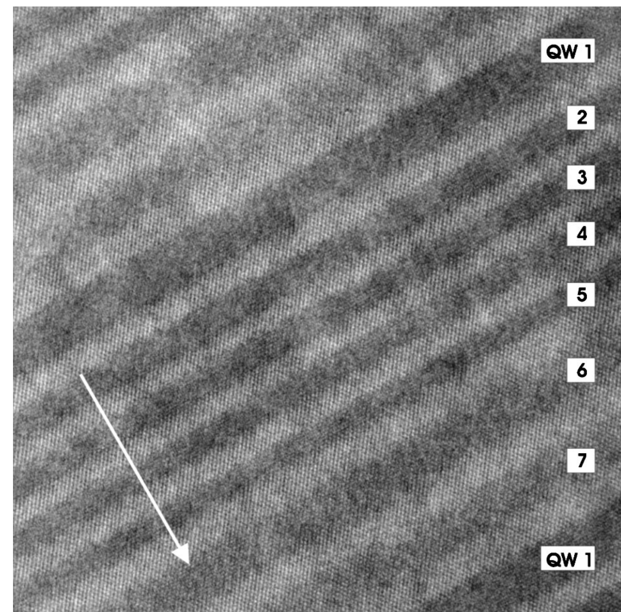

FIG. 2. TEM picture at the [110] pole of sample S1, showing one period of the cascade. The QW numbers correspond to those in Fig. 1. The arrow indicates the [001] direction. This is also the growth direction and direction of the flow of the current.

We investigated the dependence of the emission spectra on the current in sample S1. As shown in Fig. 4(a) the peak position is independent of the current. The peak broadens at the low-energy side and the integrated EL intensity [Fig. 4(b)] increases faster than linearly with an increase in cur-

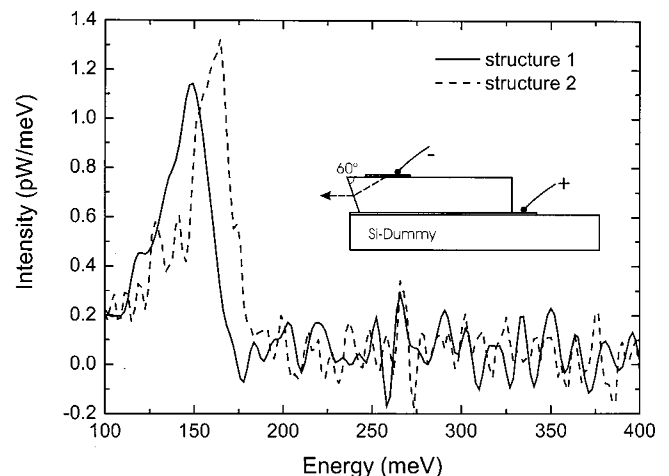

FIG. 3. Spectra of samples S1 and S2 at 20 K with 300 mA current and duty cycle of 38%. The inset shows the sample emission geometry.

Downloaded 27 Aug 2002 to 129.187.9.4. Redistribution subject to AIP license or copyright, see http://ojps.aip.org/aplo/aplcr.jsp

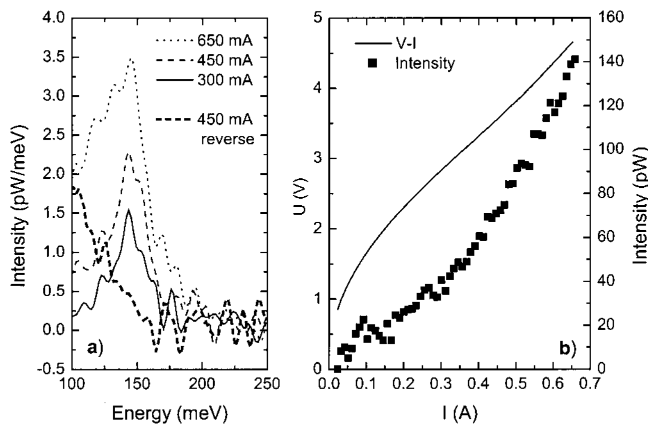

FIG. 4. (a) Current-dependent EL spectra of sample S1 and a spectrum at reverse bias at 80 K; (b) $I-V$ curve and integrated EL intensity.

rent. The low-energy broadening is attributed to radiative transitions at higher in-plane momenta k_{II} around $k_{\text{II}}=0$, which result in reduced transition energy according to the larger in-plane subband dispersion of HH1 compared to that of HH2. The $k\cdot p$ calculation results shown in Fig. 5 strongly support this. Under reverse bias the EL peak is not observed, only a thermal background is visible. This is a strong indication of the intersubband origin of the observed EL in the forward direction. The thermal background in reverse bias may also give an estimate of the thermal contributions to the EL spectra at large current in the forward direction. It may partially cause the superlinear increase in the total EL intensity with current [Fig. 4(b)].

Temperature-dependent measurements with a current of 300 mA and 37% duty cycle deliver nearly identical spectra in the temperature range from 20 to 90 K. At higher temperatures, up to 160 K, the peak is still visible but it starts to broaden towards the low-energy side while the peak height decreases. These results are also explained well by the different in plane-dispersions of HH1 and HH2.

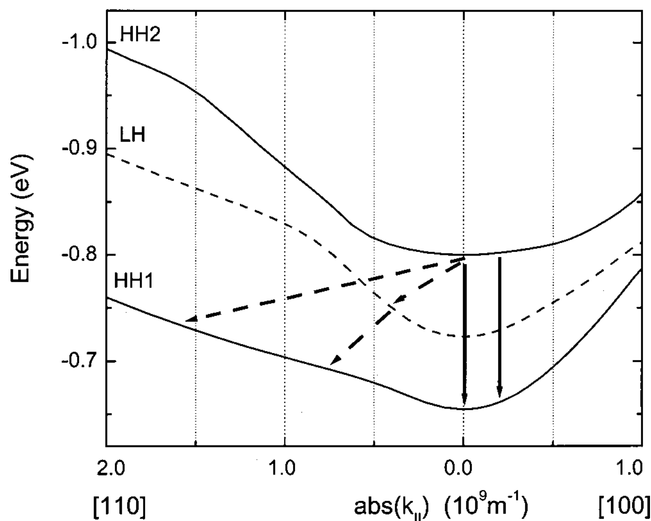

FIG. 5. In-plane subband energy dispersion in the [100] and [110] direction of the HH2, LH and HH1 subbands in the active well (QW1). The dashed arrows indicate the paths of nonradiative relaxation from the HH2 to the HH1 subband. The solid arrows mark the radiative transitions, which contribute to the EL emission.

To evaluate the main path that dominates nonradiative relaxation and thus limits the EL intensity, we calculated the hole scattering rates. Our calculations yield an overall depopulation time of 400 fs for the HH2 state. This time is longer than that found by Kaindl *et al.*[13] for a $Si_{0.5}Ge_{0.5}$ QW, but it is considerably smaller than typical values of III–V QCLs.[1,3] As indicated in Fig. 5 the HH2 state is scattered directly to HH1 states with a time constant of 614 fs at k_{II} values, where the in-plane dispersion $E(k_{\text{II}})$ band is rather flat in the [110] direction. This makes the HH2–HH1 transition faster than the cascaded transition via the LH (HH2–LH scattering time of 1170 fs), in contrast to the situation in Ref. 13.

The $I-V$ characteristic in Fig. 4(b) indicates a voltage drop of about 1.3 V across the quantum cascade (QC) structure, obtained by extrapolating the linear part of the sample resistance to the voltage axis. This gives the voltage drop caused by the nonlinear part of the sample's resistance. It corresponds to a lower limit of the electric field of 24 kV/cm in the cascades, which is noticeably smaller than the 55 kV/cm that we used to calculate the band structure. A reason for this might be that holes are able to tunnel into the neighboring QW states even at imperfect cascade alignment due to the thermal population of states at higher kinetic energy or band bending caused by charge accumulations.

In summary, we have demonstrated intersubband EL between HH subbands in two SiGe quantum cascade structures with narrow EL emission at 143 and 159 meV. The EL spectra, depending on the layer parameters, current and temperature, are described well by the band structure calculations in $k\cdot p$ formalism.

This work was financially supported by the DFG (Ab35/3-2). The authors would like to acknowledge H. Cerva of Siemens Munich for providing the TEM pictures.

[1] J. Faist, F. Capasso, D. L. Sivco, C. Sirtori, A. Hutchinson, and A. Y. Cho, Science **264**, 553 (1994).
[2] M. M. Rieger and P. Vogl, Phys. Rev. B **48**, 14276 (1993).
[3] G. Scamarcio, F. Capasso, C. Sirtori, J. Faist, A. L. Hutchinson, D. L. Sivco, and A. Y. Cho, Science **276**, 773 (1997).
[4] C. Sirtori, P. Kruck, S. Barbieri, P. Collot, J. Nagle, M. Beck, J. Faist, and U. Oesterle, Appl. Phys. Lett. **73**, 3486 (1998).
[5] G. Dehlinger, L. Diehl, U. Genser, H. Sigg, J. Faist, K. Ensslin, D. Grützmacher, and E. Müller, Science **290**, 2277 (2000).
[6] D. J. Godbey, J. V. Lill, J. Deppe, and K. D. Hobart, Appl. Phys. Lett. **65**, 711 (1994).
[7] D. J. Godbey and M. G. Ancona, Appl. Phys. Lett. **61**, 2217 (1992).
[8] S. Fukatsu, K. Fujita, H. Yaguchi, Y. Shiraki, and R. Ito, Appl. Phys. Lett. **59**, 2103 (1991).
[9] M. Woerner and T. Elsaesser, Phys. Rev. B **51**, 17490 (1995).
[10] G. Sun and L. Friedman, Phys. Rev. B **53**, 3966 (1996).
[11] B. W. Dodson and J. Y. Tsao, Appl. Phys. Lett. **51**, 1325 (1987).
[12] T. Fromherz, E. Koppensteiner, M. Helm, G. Bauer, J. F. Nützel, and G. Abstreiter, Phys. Rev. B **50**, 15073 (1994).
[13] R. A. Kaindl, M. Wurm, K. Reimann, M Woerner, T. Elsaesser, C. Miesner, K. Brunner, and G. Abstreiter, Phys. Rev. Lett. **86**, 1122 (2001).

Downloaded 27 Aug 2002 to 129.187.9.4. Redistribution subject to AIP license or copyright, see http://ojps.aip.org/aplo/aplcr.jsp